Available online at www.sciencedirect.com
ScienceDirect
Structural Safety 29 (2007) 32–48
STRUCTURAL SAFETY
www.elsevier.com/locate/strusafe

Reliability-based vector nonstationary random critical earthquake excitations for parametrically excited systems

A.M. Abbas [a,b,c], C.S. Manohar [c,*]

[a] Department of Civil Engineering, Minia University, Minia 61111, Egypt
[b] Department of Civil Engineering, Nagasaki University, Nagasaki 852-8521, Japan
[c] Department of Civil Engineering, Indian Institute of Science, Bangalore 560012, India

Received 17 April 2002; received in revised form 8 December 2004; accepted 16 November 2005
Available online 7 March 2006

Abstract

The study considers the earthquake response of stack-like structures subjected to simultaneous action of random horizontal and vertical earthquake acceleration components. The governing equation of motion in this case is approximated by a set of coupled randomly time varying ordinary differential equations. The components of earthquake accelerations are modelled as nonstationary Gaussian random processes that are obtained by multiplying deterministic modulating functions with partially specified stationary random processes. Specifically, it is assumed that the matrix of power spectral density (psd) functions of the stationary components is not known, while, the variance, average rate of zero crossings, entropy rate and frequency range of interest are taken to be known. The unknown input psd matrix is determined such that the reliability index associated with a specified structure performance function is minimized. The solution procedure employed, combines the theory of Hasofer–Lind reliability indices, response surface modelling and constrained nonlinear optimization tools. The critical input psd matrix so obtained leads to the definition of excitation models that produce the least favorable response, which, at the same time, possess a few of the well known properties of earthquake loads. A numerical example that illustrates the concepts developed with reference to a chimney structure is provided.

Keywords: Structural reliability; Critical earthquake loads; Parametric excitation; Random vibration; Nonlinear optimization; Tall structures

1. Introduction

The modelling of the effect of vertical earthquake accelerations on stack-like structures results in governing equations of motion with time varying coefficients. The study of such systems, especially, when the earthquake loads are modelled as random processes, constitutes a challenging class of problems in aseismic reliability analysis. These systems belong to the class of parametrically excited dynamical systems and their study has

* Corresponding author. Tel.: +91 80 2293 3121; fax: +91 80 2360 0404.
E-mail addresses: abbas@civil.nagasaki-u.ac.jp (A.M. Abbas), manohar@civil.iisc.ernet.in (C.S. Manohar).

0167-4730/$ - see front matter © 2006 Elsevier Ltd. All rights reserved.
doi:10.1016/j.strusafe.2005.11.003

attracted wide research attention. Thus, for instance, the monograph by Ibrahim [1] is entirely devoted to parametric random vibration problems. Similarly, the works of Bolotin [2], Dimentberg [3] and Lin and Cai [4] contain extensive information on analysis of stochastic time varying systems. In the context of earthquake engineering, a few authors have investigated the parametric actions of vertical component of the earthquake acceleration. Thus, the paper by Iyengar and Shinozuka [5] employed Monte Carlo simulations to investigate the response statistics of tall structures subjected to correlated stationary horizontal and vertical ground motions. The papers by Lin and Shih [6,7], Shih and Lin [8] and Shih and Chen [9] investigated the response of tall linear/nonlinear structures under vertical seismic loads. Similarly, Ahmadi [10] and Ahmadi and Abdel-Rahman [11] have discussed the notion of stochastic stability of frame structures subjected to parametric actions of multi-component earthquake loads. Loh and Ma [12] have investigated the formulation of a uniform hazard response spectra for structures subjected to simultaneous action of horizontal and vertical ground motions.

In the present study, the problem of earthquake response of structures driven parametrically by multi-component earthquake loads is considered from a different perspective. The viewpoint here is rooted in the concept of critical earthquake load modelling. The concept of critical earthquake loads was introduced by Drenick [13] and some of the early works in this field were by Shinozuka [14] and Iyengar [15]. The basic premise in developing these models is the assumption that complete information on earthquake loads, that would enable the analyst to carry out a desired response/reliability analysis, is often not available. Instead, what would be available is only a partial description of the loads. The method proposes that a complete model for the inputs be arrived at by maximizing the structural response under constraints that reflect the known features of the earthquake loads. Thus, these models are tailor made to produce the highest response, and, therefore, provide an idea on the worst that could happen to the structure when inputs are specified only partially.

In the context of probabilistic earthquake load modelling, a few authors have studied critical excitation modelling. Thus, Iyengar and Manohar [16] considered single point earthquake loads modelled as partially specified nonstationary Gaussian random processes. The input power spectral density (psd) functions, that produced highest response variance in linear systems with constraints on total average input energy, were obtained as solutions of an algebraic eigenvalue problem. Srinivasan et al. [17] modelled earthquake loads as nonstationary filtered shot noise processes and optimized the parameters of the models so as to produce highest response variance. Manohar and Sarkar [18] and Abbas and Manohar [19] imposed constraints on input variance, average zero crossing rate and entropy rate. The consideration of input entropy rate was brought in to impart the observed levels of disorder in the recorded earthquake accelerograms. In a series of recent studies Takewaki [20,21] has studied critical psd function models for earthquake loads for linear and nonlinear systems. This author has introduced constraints on the peak of input psd function. Studies on spatially varying critical earthquake excitations have been conducted by Sarkar and Manohar [22,23] and Abbas and Manohar [24]. In these studies the optimal earthquake psd matrix models for vector random excitations have been obtained by maximizing response variance. Sarkar and Khajehpour [25] model the critical acceleration as a stationary Gaussian random process with an unknown psd function, which is computed such that the mean of the level crossing rate of response of a given linear structure as well as the input entropy rate, are maximized under a constraint on the input variance. More recently, the present authors, in a two-part paper, have explored the use of methods of structural reliability analysis in deriving critical earthquake excitations for linear and nonlinear structures [26,27]. The critical excitations in these studies were defined as those that maximize the structure probability of failure over a given period of time.

In the context of structures driven parametrically by multi-component earthquake loads, to the best of authors' knowledge, there exists no study that aims to develop critical earthquake load models for these systems. The present study aims to address this problem. With this in view, the earthquake response of a stack-like structure subjected to the simultaneous action of horizontal and vertical earthquake accelerations is considered. The transverse bending of the stack is investigated by including the effects of horizontal acceleration, self-weight and parametric excitation induced by the vertical acceleration. The two components of the earthquake ground acceleration are modelled as a vector of correlated nonstationary random processes each of which is obtained as a product of a deterministic time envelope and a zero mean, stationary Gaussian random processes. The stationary components are furthermore taken to be jointly stationary and jointly Gaussian. The knowledge on the input is restricted to the average total energy, zero crossing rates and entropy rates

of the individual components. The psd matrix of the stationary components of the excitation vector is taken to be unknown and this is required to be determined so that a measure of the structural response is maximized. In choosing the response variable to be maximized it is to be noted that response displacement (or any linear function of displacement, such as stress component at a point or stress resultant at a cross-section) of linear parametrically excited systems could have non-zero mean and would be non-Gaussian in nature even when the inputs are Gaussian. This would mean that critical excitations that maximize response variance are of limited interest, since, these excitations need not have to maximize the mean response. Another important factor to be noted is that response moments or the response probability density function of systems under parametric and external random excitations, in general, cannot be determined exactly. This difficulty can be overcome by resorting to approximate methods of response analysis such as those based on closure approximations on the moment equations or using an assumed non-Gaussian probability density function [1,28]. It was found in our studies that procedures to determine critical excitations based on these approximations lead to unwieldy computational demands. In the present study we report on an alternative strategy to proceed further. This is based on the use of methods of structural reliability. Accordingly, the study introduces a performance function that defines acceptable limits on structural response. The critical input psd matrix is now defined as that which minimizes the Hasofer–Lind reliability index associated with this performance function. The evaluation of the reliability index, in turn, is based on the use of response surface modelling of failure surface near the check point. A numerical example that illustrates the details of the formulations developed is presented with reference to the determination of critical psd matrix for a tall chimney structure.

2. A stack subjected to vertical and horizontal earthquake loads

Fig. 1 shows a stack-like structure subjected to one horizontal and one vertical component of earthquake load. The equilibrium equation for the structure can be shown to be given by [5]

$$\frac{\partial^2}{\partial y^2}\left\{\mathrm{EI}(y)\frac{\partial^2 W(y,t)}{\partial y^2}+[g+\ddot{y}_g(t)]\int_y^h m(\xi)[W(\xi,t)-W(y,t)]\,\mathrm{d}\xi\right\} + m(y)\frac{\partial^2 W(y,t)}{\partial t^2}+C\frac{\partial}{\partial t}[W(y,t)-x_g(t)]=0 \tag{1}$$

Here, $W(y,t)$ is the total displacement, $x_g(t)$ is the horizontal ground displacement, $\ddot{y}_g(t)$ is the vertical ground acceleration, EI(y) is the flexural rigidity, h is the total height of the structure, $m(y)$ is the mass per unit length, C is the damping coefficient, y is the spatial coordinate and g is the acceleration due to gravity. The boundary conditions associated with the above equation of motion are given by $W(0,t)=x_g(t)$, $\left.\frac{\partial W(y,t)}{\partial y}\right|_{y=0}=0$, $\mathrm{EI}\left.\frac{\partial^2 W(y,t)}{\partial y^2}\right|_{y=h}=0$ and $\mathrm{EI}\left.\frac{\partial^3 W(y,t)}{\partial y^3}\right|_{y=h}=0$. Assuming the mass and flexural rigidity to be constant along y, and, carrying out necessary reductions, the above equation can be recast as

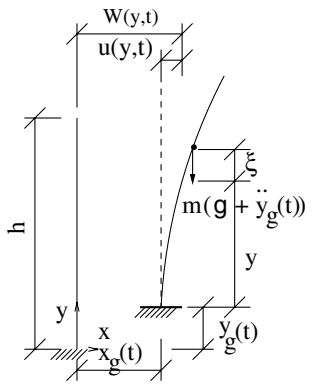

Fig. 1. Example structure considered.

$$\mathrm{EI}\frac{\partial^4 W(y,t)}{\partial y^4}+m[g+\ddot{y}_g(t)]\left\{(y-h)\frac{\partial^2 W(y,t)}{\partial y^2}+\frac{\partial W(y,t)}{\partial y}\right\}+m\ddot{W}(y,t)+C[\dot{W}(y,t)-\dot{x}_g(t)]=0 \tag{2}$$

This equation constitutes a partial differential equation with time varying coefficients and time varying boundary conditions. A first step in analyzing dynamical systems with this type of equations of motion, would be to introduce the transformation $W(y,t)=u(y,t)+x_g(t)$. Here, $u(y,t)$ can be viewed as the relative displacement of the structure. Consequent to this transformation, the field equation reads

$$\mathrm{EI}\frac{\partial^4 u(y,t)}{\partial y^4}+m[g+\ddot{y}_g(t)]\left\{(y-h)\frac{\partial^2 u(y,t)}{\partial y^2}+\frac{\partial u(y,t)}{\partial y}\right\}+m\ddot{u}(y,t)+C\dot{u}(y,t)=-m\ddot{x}_g(t) \tag{3}$$

Accordingly, the set of boundary conditions given above, reduces to $u(0,t)=0$, $\left.\frac{\partial u(y,t)}{\partial y}\right|_{y=0}=0$, $\left.\mathrm{EI}\frac{\partial^2 u(y,t)}{\partial y^2}\right|_{y=h}=0$ and $\left.\mathrm{EI}\frac{\partial^3 u(y,t)}{\partial y^3}\right|_{y=h}=0$. Thus, the effect of the transformation employed here, is seen to make the boundary conditions time invariant. This enables the construction of approximate series solution to Eq. (3) given by

$$u(y,t)=\lim_{N\to\infty}\sum_{i=1}^{N}\phi_i(y)q_i(t) \tag{4}$$

Here $\{\phi_i(y)\}_{i=1}^{\infty}$ are the trial functions. In the present study we take these functions to coincide with the undamped eigenfunctions of a cantilever beam of height h, flexural rigidity EI and mass per unit length m. These functions, as is well known, satisfy all the relevant boundary conditions (namely, $\phi_i(0)=0$, $\left.\frac{\partial\phi_i(y)}{\partial y}\right|_{y=0}=0$, $\left.\frac{\partial^2\phi_i(y)}{\partial y^2}\right|_{y=h}=0$ and $\left.\frac{\partial^3\phi_i(y)}{\partial y^3}\right|_{y=h}=0$), are continuous over $[0,h]$, differentiable at least up to the fourth order, and form a complete set of orthogonal functions. Consequently, $u(y,t)$ can be represented with any desired accuracy by increasing the number of terms in the series representation in Eq. (4); see, the book by Finlayson [29], for a discussion on questions of convergence of representation used in Eq. (4). Furthermore, these conditions also permit interchange of summation and differentiation operations; see, the book by Flatto [30] for the relevant mathematical details. The functions $\{\phi_i(y)\}_{i=1}^{\infty}$ are known to be given by [31]

$$\phi_i(y)=\cosh\lambda_i y-\cos\lambda_i y-\frac{\sinh\lambda_i-\sin\lambda_i}{\cosh\lambda_i+\cos\lambda_i}(\sinh\lambda_i y-\sin\lambda_i y) \tag{5}$$

where, the first few of the λs are given by $\lambda_1=1.87510407$, $\lambda_2=4.69409113$ and $\lambda_3=7.85475744$. Substituting Eq. (4) into Eq. (3), one gets the residue

$$\begin{aligned}\varepsilon(y,t)=&\mathrm{EI}\sum_{n=1}^{\infty}\frac{\partial^4\phi_n(y)}{\partial y^4}q_n(t)+m[g+\ddot{y}_g(t)]\left\{(y-h)\sum_{n=1}^{\infty}\frac{\partial^2\phi_n(y)}{\partial y^2}q_n(t)+\sum_{n=1}^{\infty}\frac{\partial\phi_n(y)}{\partial y}q_n(t)\right\}\\&+m\sum_{n=1}^{\infty}\phi_n(y)\ddot{q}_n(t)+C\sum_{n=1}^{\infty}\phi_n(y)\dot{q}_n(t)+m\ddot{x}_g(t)\end{aligned} \tag{6}$$

According to the Galerkin approximation, $\varepsilon(y,t)$ is taken to be orthogonal to the trial functions, and, thus one gets $\int_0^h \varepsilon(y,t)\ \phi_i(y)\mathrm{d}y=0,\ i=1,2,\ldots,\infty$. This leads to the governing equations of motion for the generalized coordinates, $q_i(t)$, $(i=1,2,\ldots,\infty)$ given by

$$\ddot{q}_i(t)+2\zeta_i\omega_i\dot{q}_i(t)+\omega_i^2 q_i(t)+\frac{g+\ddot{y}_g(t)}{h}\sum_{j=1}^{\infty}\alpha_{ij}q_j(t)=-k_i\ddot{x}_g(t);\quad i=1,2,\ldots,\infty \tag{7}$$

Here, ω_i is the ith natural frequency of the structure and α_{ij} and k_i are constants given by [31]

$$\omega_i=\frac{\lambda_i^2}{2\pi h^2}\sqrt{\frac{\mathrm{EI}}{m}}\quad \alpha_{ij}=\int_0^h\left\{(y-h)\frac{\partial^2\phi_i(y)}{\partial y^2}+\frac{\partial\phi_i(y)}{\partial y}\right\}\phi_j(y)\,\mathrm{d}y;\quad k_i=\frac{\int_0^h\phi_i(y)\,\mathrm{d}y}{h};\quad i\neq j=1,2,\ldots,\infty \tag{8}$$

Assuming that the system starts from rest, it can be shown that the set of initial conditions associated with the above equations of motion (Eq. (7)) in the generalized coordinates are given by $q_i(0)=0$, $\dot{q}_i(0)=0$, $i=1,2,\ldots,\infty$. It is clearly seen that equations governing $q_i(t)$, $(i=1,2,\ldots,\infty)$ (Eq. (7)) are mutually coupled

through terms involving the vertical acceleration and self-weight of the structure. The infinite sum appearing in the left hand side of this equation needs to be appropriately truncated in the numerical solution.

3. Probabilistic critical earthquake loads

We begin by modelling the horizontal and the vertical ground accelerations as a pair of correlated non-stationary Gaussian random processes. These processes are further represented as $\ddot{x}_g(t) = e_x(t)\ddot{w}_g(t)$ and $\ddot{y}_g(t) = e_y(t)\ddot{v}_g(t)$, where, $e_x(t)$ and $e_y(t)$ are the deterministic enveloping functions, given by

$$\begin{aligned} e_x(t) &= A_{0x}[\exp(-\alpha_{x_1}t) - \exp(-\alpha_{x_2}t)] \quad \alpha_{x_2} > \alpha_{x_1} > 0 \\ e_y(t) &= A_{0y}[\exp(-\alpha_{y_1}t) - \exp(-\alpha_{y_2}t)] \quad \alpha_{y_2} > \alpha_{y_1} > 0 \end{aligned} \tag{9}$$

The processes $\ddot{w}_g(t)$ and $\ddot{v}_g(t)$ are taken to constitute a vector of jointly stationary Gaussian random processes with zero mean and an unspecified psd matrix. It is aimed to determine this psd matrix such that the resulting earthquake input produces the most unfavorable structural system performance. To arrive at an acceptable structural performance criterion we first note that the structural response under combined horizontal and vertical earthquake loads has a non-zero mean and is non-Gaussian in nature. Consequently, it becomes meaningful to specify the structural performance in terms of measures of the highest response. Thus, we propose a performance function of the form

$$g[R, z\{y_0, t, \ddot{w}_g(t), \ddot{v}_g(t)\}] = R - \max_{0<t<\infty} |z(y_0, t)| \tag{10}$$

Here, R is the permissible limit on the structural response $\max|z(y,t)|$ at $y = y_0$ and $0 < t < \infty$ and the quantity $z(y,t)$ could be the displacement response, stress components or stress resultants. The probability of structural failure, as per this performance criterion, is given by $P_f = P[R - \max_{0<t<\infty}|z(y_0,t)| < 0]$. The determination of this probability of failure constitutes a problem in time-variant reliability analysis. To determine the unknown input psd matrix of the vector $[\ddot{w}_g(t), \ddot{v}_g(t)]^t$, we propose that this unknown psd matrix be such that the probability of structural failure, defined above, is maximized under a set of constraints reflecting known characteristics of the ground accelerations vector $[\ddot{x}_g(t), \ddot{y}_g(t)]^t$. It must be noted in this context that the probability distribution function of the quantity $\max_{0<t<\infty}|z(y_0,t)|$ is generally not deducible for system governed by Eq. (7). To proceed further, we can make closure approximations to analyze Eq. (7) on the lines suggested by Iyengar and Dash [28] and Ibrahim [1]. While these methods can be considered to be useful in approximating the response moments, their usefulness in computing failure probabilities and extreme value statistics of the response is, however, not well established. An alternative in this context would be to adopt first order reliability methods combined with response surface methods to indirectly characterize the failure probability. In the present study, we adopt this latter approach.

The response surface methods for reliability assessment are basically meant for treatment of situations in which performance functions are implicitly available in terms of a set of random variables. See, for example, the papers by Faravelli [32], Bucher and Bourgund [33] and Rajashekhar and Ellingwood [34] for basic expositions of the response surface modeling in structural reliability analysis. These methods typically enable the determination of the Hasofer–Lind reliability index associated with the given performance function. It may recalled in this context that the knowledge of the Hasofer–Lind reliability index generally does not lead to the exact determination of the reliability of the structure. Nevertheless, it is known that the index possesses the orderability characteristic which ensures that an increase in this index implies an increase in the true reliability of the system. Thus, in the context of development of critical excitation models, it is of significance to note that a lowering of the reliability index indirectly implies an increase in the true failure probability. Furthermore, the reliability index based methods are essentially applicable to problems in which performance functions are dependent on a set of random variables as in static problems. In the present study, the performance function (Eq. (10)) is implicitly dependent upon the random processes $\ddot{w}_g(t)$ and $\ddot{v}_g(t)$. To facilitate the application of response surface modelling, we represent these processes in terms of a pair of Fourier series given by

$$\ddot{w}_g(t) = \sum_{n=1}^{N_f} A_n \cos\Omega_n t + B_n \sin\Omega_n t; \quad \ddot{v}_g(t) = \sum_{n=1}^{N_f} C_n \cos\Omega_n t + D_n \sin\Omega_n t \tag{11}$$

The coefficients $\{A_n, B_n, C_n, D_n\}_{n=1}^{N_f}$ here, are taken to be a vector of zero mean Gaussian random variables. Since the processes $\ddot{w}_g(t)$ and $\ddot{v}_g(t)$ are taken to be jointly stationary, it emerges that these random variables must be such that

$$\langle A_m A_n\rangle = \langle B_m B_n\rangle = \sigma_{wn}^2\delta_{mn}; \quad \langle C_m C_n\rangle = \langle D_m D_n\rangle = \sigma_{vn}^2\delta_{mn}; \quad \langle A_m B_n\rangle = \langle C_m D_n\rangle = 0 \tag{12}$$

$$\langle A_m C_n\rangle = \langle B_m D_n\rangle = \sigma_{ACn}\delta_{mn}; \quad \langle A_m D_n\rangle = -\langle B_m C_n\rangle = \sigma_{ADn}\delta_{mn}; \quad \forall m,n = 1,2,\ldots,N_f \tag{13}$$

It is to be noted that, the conditions given by Eq. (12) guarantee that the processes $\ddot{w}_g(t)$ and $\ddot{v}_g(t)$ are individually stationary in nature, while those of Eq. (13) ensure that $\ddot{w}_g(t)$ and $\ddot{v}_g(t)$ are jointly stationary. Consistent with these requirements, the auto covariance and cross covariance functions of these processes can be shown to be given by

$$R_{ww}(\tau) = \sum_{n=1}^{N_f}\sigma_{wn}^2\cos\Omega_n\tau; \quad R_{vv}(\tau) = \sum_{n=1}^{N_f}\sigma_{vn}^2\cos\Omega_n\tau; \quad R_{wv}(\tau) = \sum_{n=1}^{N_f}\sigma_{ACn}\cos\Omega_n\tau + \sigma_{ADn}\sin\Omega_n\tau \tag{14}$$

It follows that $R_{ww}(\tau) = R_{ww}(-\tau)$, $R_{vv}(\tau) = R_{vv}(-\tau)$ and $R_{wv}(\tau) = R_{vw}(-\tau)$ which are as they must be. The performance function given by Eq. (10) can now be recast as

$$g[R,\{A_n,B_n,C_n,D_n\}_{n=1}^{N_f}] = R - \max_{0<t<\infty}|z(y_0,t,\{A_n,B_n,C_n,D_n\}_{n=1}^{N_f})| \tag{15}$$

It must be noted that an explicit expression for $\max_{0<t<\infty}|z(y_0,t,\{A_n,B_n,C_n,D_n\}_{n=1}^{N_f})|$ in terms of the variables $\{A_n,B_n,C_n,D_n\}_{n=1}^{N_f}$ is not derivable. What is, in fact, available is the governing differential equations of motion, given by

$$\ddot{q}_i(t) + 2\zeta_i\omega_i\dot{q}_i(t) + \omega_i^2 q_i(t) + \frac{1}{h}\left\{g + e_y(t)\left[\sum_{n=1}^{N_f}A_n\cos\Omega_n t + B_n\sin\Omega_n t\right]\right\}\sum_{j=1}^{\infty}\alpha_{ij}q_j(t)$$

$$= -k_i e_x(t)\left[\sum_{n=1}^{N_f}C_n\cos\Omega_n t + D_n\sin\Omega_n t\right]; \quad i = 1,2,\ldots,\infty \tag{16}$$

that implicitly relates the performance function $g[R,\{A_n,B_n,C_n,D_n\}_{n=1}^{N_f}]$ with the variables R and $\{A_n,B_n,C_n,D_n\}_{n=1}^{N_f}$. Consequently, analytical methods of reliability assessment, based on the use of reliability indices, cannot be directly applied to analyze this problem. To proceed further, we resort to the response surface methods. Thus, we redefine the problem of finding critical earthquake excitations as computing the variables $\{\sigma_{wn}^2,\ \sigma_{vn}^2,\ \sigma_{ACn},\ \sigma_{ADn}\}_{n=1}^{N_f}$, such that the Hasofer–Lind reliability index, β_{HL}, associated with the performance function as given in Eq. (15), is minimized subjected to a set of constraints that reflects known feature of the inputs. These constraints, in terms of $\{\sigma_{wn}^2,\ \sigma_{vn}^2,\ \sigma_{ACn},\ \sigma_{ADn}\}_{n=1}^{N_f}$, are taken to be given by Manohar and Sarkar [18] and Abbas and Manohar [19]

$$\sum_{n=1}^{N_f}\sigma_{wn}^2 = E_{0x}; \quad \sum_{n=1}^{N_f}\sigma_{vn}^2 = E_{0y} \tag{17}$$

$$\sum_{n=1}^{N_f}\sigma_{wn}^2\Omega_n^2 = E_{2x}; \quad \sum_{n=1}^{N_f}\sigma_{vn}^2\Omega_n^2 = E_{2y} \tag{18}$$

$$\sigma_{ACn}^2 + \sigma_{ADn}^2 < \sigma_{wn}^2 + \sigma_{vn}^2 \quad n = 1,2,\ldots,N_f \tag{19}$$

$$\sigma_{wn}^2 > 0; \quad \sigma_{vn}^2 > 0; \quad n = 1,2,\ldots,N_f \tag{20}$$

$$\frac{1}{2(\omega_c-\omega_0)}\sum_{n=1}^{N_f}(\Omega_n-\Omega_{n-1})\log_e\left[1.0+\frac{\sigma_{wn}^2}{S_0(\Omega_n-\Omega_{n-1})}\right] \geqslant \Delta\overline{H}_{Wx}$$

$$\frac{1}{2(\omega_c-\omega_0)}\sum_{n=1}^{N_f}(\Omega_n-\Omega_{n-1})\log_e\left[1.0+\frac{\sigma_{vn}^2}{S_0(\Omega_n-\Omega_{n-1})}\right] \geqslant \Delta\overline{H}_{Wy} \tag{21}$$

These constraints are basically of two types: the first, contained in Eqs. (17), (18), and (21), is related to the known features of earthquake, and, the second, contained in Eqs. (19) and (20), essentially specify

mathematical requirements, such as, non-negativity of variance and positive definiteness of covariance matrix. Clearly, the second type of constraints are independent of the seismic region and soil condition.

Thus, Eq. (17) represents bounds on the input total energy; Eq. (18), along with Eq. (17), define the constraints on the input zero crossings rate. The constraints in Eq. (19) can be shown to be equivalent to the requirement that the covariance matrix of $\{A_n, B_n, C_n, D_n\}$ is positive definite for all n. Similarly, Eq. (20) states the requirement that the psd function is positive. The last set of constraints, given in Eq. (21), represent lower bounds on the input entropy rate. In this context, it may be recalled that, for a zero mean, band limited, stationary Gaussian random process $\xi(t)$ with psd function $S(\omega)$, the entropy rate is given by Papoulis and Pillai [35]

$$\overline{H} = \log_e \sqrt{2\pi e} + \frac{1}{2(\omega_2 - \omega_1)} \int_{\omega_1}^{\omega_2} \log_e S(\omega)\, \mathrm{d}\omega \tag{22}$$

Here (ω_1, ω_2) is the frequency bandwidth. One would face serious computational difficulties in computing $\overline{H}$, if $S(\omega)$ approaches zero for some ω in (ω_1, ω_2). To circumvent this difficulty, one can define a reference white noise with intensity I and calculate the change in the entropy rate of $\xi(t)$ when this white noise is added to $\xi(t)$. It can be shown that this increase in entropy rate is given by

$$\Delta\overline{H} = \int_{\omega_1}^{\omega_2} \log_e \left[1 + \frac{S(\omega)}{I}\right] \mathrm{d}\omega \tag{23}$$

The formulation of constraints, as stated in Eq. (21), is based on these considerations. Furthermore, as has been already noted, the relevance of introducing the entropy rate concepts into the definition of critical excitations has been explained in the works of Manohar and Sarkar [18] and Abbas and Manohar [19]. These authors have noted that, in the absence of these constraints, the resulting critical excitations become nearly deterministic in nature and produce conservative estimates of critical response. The near deterministic nature of the critical excitations here is manifest in terms of the critical psd functions being highly narrow banded with average power getting concentrated at the system natural frequencies. The associated samples of excitation time histories would be poor in frequency content and display nearly sinusoidal behavior. Such 'ordered' excitations would hardly serve as valid models for earthquake inputs. This points towards the fact that the prior knowledge of earthquake records as being random in nature has not been made adequate use of in defining the critical excitations. The notion of entropy rate overcomes this limitation and this notion here essentially enables quantification of amount of disorder that one might expect in a realistic earthquake. It may also be noted in this context that entropy based principles offer powerful modelling tools in the treatment of random phenomena with incompletely specified probability space: see, for example the comprehensive monograph by Kapur [36] on this topic. Given that the concept that random critical excitation essentially deals with incompletely specified random processes it is reasonable to expect that the concept of entropy has bearing on the development of these models. Clearly, the problem of finding the critical psd matrix is that of a constrained nonlinear optimization and is solved by using the sequential quadratic programming (SQP) method, through the '*CONSTR*' program of the Matlab Optimization Toolbox.

In the numerical work, the quantities E_{0x}, E_{0y}, E_{2x}, E_{2y}, $\Delta\overline{H}_{Wx}$ and $\Delta\overline{H}_{Wy}$ are estimated using past recorded earthquake data. The quantities E_{0x} and E_{0y} are taken as the extreme values of the associated parameters across the set of past recorded ground motions. The parameters that define zero crossing rates and entropy rates (E_{2x}, E_{2y}, $\Delta\overline{H}_{Wx}$ and $\Delta\overline{H}_{Wy}$) are taken as average values from past records. This approach is considered to be consistent with the aspirations of the ground motion models that are commonly used by engineers, which, basically aim to replicate some of the gross features of recorded motions, such as, amplitude, frequency content, nonstationarity, local soil amplification effects, and duration. It is of interest to note in this context that, predictive or physical models for ground motions, which take into account several details, such as, fault dimension, fault orientation, rupture velocity, magnitude of earthquake, attenuation, stress drop, density of the intervening medium, local soil condition and epicentral distance, have also been developed in the existing literature, mainly by the seismologists [37–40]. In using these models, the engineers need to input values for a host of parameters and the success of the model depends upon how realistically this is done. It is possible to formulate the critical excitation models based on the latter class of models in which one can aim to optimize

the parameters of the model so as to realize the least favorable conditions. It is important to note that the class of admissible functions, in the determination of critical excitations, in this case, becomes further constrained by the choice that one makes for the physical model. The approach adopted in our study, in this sense, is non-parametric in nature. A comparison of results based on this approach with those from 'model based' approaches is of interest; however, we have not considered these questions in the present study.

4. Determination of critical psd matrix using response surface models

The performance function, as given by Eq. (15), is defined in the space of $4N_f$ random variables denoted collectively by the vector $\mathbf{X} = [\{A_n, B_n, C_n, D_n\}_{n=1}^{N_f}]^t$; here t denotes the matrix transposition. While it is possible to treat R also as a random variable, this possibility, however, is not considered herein. The first step in implementing the response surface method for reliability computation consists of transforming the basic random variables $\mathbf{X}$ into a vector of standard normal random variables denoted by $\mathbf{Y}$. The essence of the response surface method consists of replacing the implicit performance function, given in Eq. (15), by an approximating quadratic surface [33]

$$\bar{g}(\mathbf{Y}) = a + \sum_{i=1}^{N_{rv}} b_i Y_i + \sum_{i=1}^{N_{rv}} c_i Y_i^2 \tag{24}$$

Here $N_{rv} = 4N_f$ is the number of basic random variables on which the performance function depends and $a, \{b_i\}_{i=1}^{N_{rv}}, \{c_i\}_{i=1}^{N_{rv}}$ are the unknown deterministic parameters to be determined. The form of the response surface assumed herein does not take into account cross quadratic terms. The inclusion of these terms would lead to considerable increase in the computational efforts although the framework for solution remains essentially unaltered. The influence of this assumption on the critical response and input models is examined later in the paper. It must also be noted here that the problem of determination of the Hasofer–Lind reliability index β_{HL} itself constitutes a constrained nonlinear optimization problem [41]. This optimization problem, in turn, is embedded into the optimization problem associated with the determination of the critical psd matrix parameters. Consequently, the algorithm proposed in the present study for computing the critical input psd matrix, has two optimization routines. The first routine is meant for computing the critical excitations, while the second subroutine, that computes β_{HL}, is called by the main routine at each major step of computing the critical input. The steps involved in these calculations are as follows:

1. Select a failure criterion for the structure, fix R, define mean and variance of the basic random variables, $\{\mu_i, \sigma_i^2\}_{i=1}^{N_{rv}}$, and make an initial guess for the optimization variables $\{\sigma_{wn}^2,\ \sigma_{vn}^2,\ \sigma_{ACn},\ \sigma_{ADn}\}_{n=1}^{N_f}$.
2. Define the performance function $g(R,\ \{A_n, B_n, C_n, D_n\}_{n=1}^{N_f})$ as given by Eq. (15).
3. Make an initial guess for the failure point $\{x_{i0}^*\}_{i=1}^{N_{rv}}$ and compute the corresponding point in the standard uncorrelated normal space, $\{y_{i0}^*\}_{i=1}^{N_{rv}}$. Here, the transformation $\mathbf{Y} = \mathbf{T}^t\mathbf{X}'$ is used, where, $X_i' = \frac{X_i - \mu_i}{\sigma_i}$, is the reduced variate and $\mathbf{T}$ is an orthogonal transformation matrix. The details of this transformation are provided in the book by Ang and Tang [42].
4. Call the basic optimization routine that provides new values for $\{\sigma_{wn}^2,\ \sigma_{vn}^2,\ \sigma_{ACn},\ \sigma_{ADn}\}_{n=1}^{N_f}$.
5. Fit a response surface in the uncorrelated standard normal space. Thus, the actual implicit performance function, $g(\mathbf{Y})$, is approximated with a closed form function $\bar{g}(\mathbf{Y})$ at the failure point. In the present work, we use a quadratic polynomial function as given in Eq. (24) [33]. The steps of this fitting are summarized as follows:
   - Sample Y in Eq. (24) at $2N_{rv} + 1$ points, that is, at mean, $\bar{\mu}_i$, and mean $\pm f\bar{\sigma}_i$ of these random variables. Here, f is a constant and $\bar{\mu}_i = 0$, $\bar{\sigma}_i = 1$ are mean and standard deviation of Y_i, respectively.
   - Evaluate the actual performance function, $g(\mathbf{Y})$ at the $2N_{rv} + 1$ points. Here, the quantity $\max_{0<t<\infty}|z(y_0, t, A_n, B_n, C_n, D_n)|$, $n = 1, 2, \ldots, N_f$, is computed using numerical integration of the governing equations of motion.
   - Solve the set of $2N_{rv} + 1$ algebraic equations given by $\mathbf{AB} = \mathbf{G}$, to compute the values of the variables $\{a, b_i, c_i\}_{i=1}^{N_{rv}}$. Here, the matrix $\mathbf{A}$ is of size $2N_{rv} + 1$ by $2N_{rv} + 1$, the matrices $\mathbf{B}$ and $\mathbf{G}$ are of the size $2N_{rv} + 1$ by 1, and these matrices are given as

$$\mathbf{A}=\begin{bmatrix}
1 & \bar{\mu}_1 & \bar{\mu}_2 & \dots & \bar{\mu}_{N_{rv}} & \bar{\mu}_1^2 & \bar{\mu}_2^2 & \dots & \bar{\mu}_{N_{rv}}^2 \\
1 & \bar{\mu}_1+f\bar{\sigma}_1 & \bar{\mu}_2 & \dots & \bar{\mu}_{N_{rv}} & (\bar{\mu}_1+f\bar{\sigma}_1)^2 & \bar{\mu}_2^2 & \dots & \bar{\mu}_{N_{rv}}^2 \\
1 & \bar{\mu}_1 & \bar{\mu}_2+f\bar{\sigma}_2 & \dots & \bar{\mu}_{N_{rv}} & \bar{\mu}_1^2 & (\bar{\mu}_2+f\bar{\sigma}_2)^2 & \dots & \bar{\mu}_{N_{rv}}^2 \\
1 & \bar{\mu}_1 & \bar{\mu}_2 & \dots & \bar{\mu}_{N_{rv}}+f\bar{\sigma}_{N_{rv}} & \bar{\mu}_1^2 & \bar{\mu}_2^2 & \dots & (\bar{\mu}_{N_{rv}}+f\bar{\sigma}_{N_{rv}})^2 \\
1 & \bar{\mu}_1-f\bar{\sigma}_1 & \bar{\mu}_2 & \dots & \bar{\mu}_{N_{rv}} & (\bar{\mu}_1-f\bar{\sigma}_1)^2 & \bar{\mu}_2^2 & \dots & \bar{\mu}_{N_{rv}}^2 \\
1 & \bar{\mu}_1 & \bar{\mu}_2-f\bar{\sigma}_2 & \dots & \bar{\mu}_{N_{rv}} & \bar{\mu}_1^2 & (\bar{\mu}_2-f\bar{\sigma}_2)^2 & \dots & \bar{\mu}_{N_{rv}}^2 \\
1 & \bar{\mu}_1 & \bar{\mu}_2 & \dots & \bar{\mu}_{N_{rv}}-f\bar{\sigma}_{N_{rv}} & \bar{\mu}_1^2 & \bar{\mu}_2^2 & \dots & (\bar{\mu}_{N_{rv}}-f\bar{\sigma}_{N_{rv}})^2
\end{bmatrix};$$

$$\mathbf{B}=[ab_1b_2\dots b_{N_{rv}}c_1c_2\dots c_{N_{rv}}]^{\mathrm{t}};\quad \mathbf{G}=[g_1(\mathbf{X}')g_2(\mathbf{X}')g_3(\mathbf{X}')\dots g_{2N_{rv}+1}(\mathbf{X}')]^{\mathrm{t}} \tag{25}$$

6. Use the explicit limit surface $\bar{g}(\mathbf{Y})$ to calculate the reliability index, β_{HL}, and design point $\{y_i^*\}_{i=1}^{N_{rv}}$. The procedures for these calculations are standard and the details of these computations are provided in Refs. [41–43]. This includes iterative calculation of the reliability index, evaluation of the performance function and updating the check-point. The subroutine is stopped when the convergence criteria $|\beta_{\mathrm{HL}_j}-\beta_{\mathrm{HL}_{j-1}}|\leqslant\delta_1$ and $|g_j(\mathbf{Y})|\leqslant\delta_2$ are satisfied. Here, δ_1 and δ_2 are small quantities to be selected.
7. Update the starting point, $\{\bar{\mu}_i\}_{i=1}^{2N_{rv}+1}$ to $\{y_{M_i}\}_{i=1}^{2N_{rv}+1}$ as $y_{M_i}=\bar{\mu}_i+(y_i^*-\bar{\mu}_i)\frac{g(\bar{\mu}_i)}{g(\bar{\mu}_i)-g(y_i^*)}$ and re-fit a new response surface using the new updated point.
8. Check convergence of the basic optimization routine, $|g_j(Y)|\leqslant|\delta_2,\ |\sigma^2_{wn_{j+1}}-\sigma^2_{wn_j}|\leqslant\delta_3,\dots,|\sigma_{ADn_{j+1}}-\sigma^2_{ADn_j}|\leqslant\delta_3$. If convergence is achieved go to next step, if not go to step 4.
9. Store the quantities, $\{\sigma^2_{wn},\ \sigma^2_{vn},\ \sigma_{ACn},\ \sigma_{ADn}\}_{n=1}^{N_{\mathrm{f}}},\ \beta_{\mathrm{HL}},\ \{x_i^*\}_{i=1}^{N_{rv}}$ and $\{\alpha_i\}_{i=1}^{N_{rv}}$.

It is of interest to note that the formulation of critical excitations in terms of optimal reliability indices, as developed above, leads to the following input-response descriptors:

- Critical psd matrix that produces the least β_{HL} that is compatible with a set of specified constraints.
- The reliability index, β_{HL}, associated with the critical input as obtained above.
- A notional probability of failure, given by $P_{\mathrm{f}_0}=\Phi(-\beta_{\mathrm{HL}})$, associated with the performance function considered. Here, $\Phi(\cdot)$ is the standard Gaussian probability distribution function.
- A check point which defines a single vector of time histories that leads to the maximum likelihood of failure, given by:

$$\ddot{x}_{\mathrm{g}}^*(t)=e_x(t)\left\{\sum_{n=1}^{N_{\mathrm{f}}}A_n^*\cos\Omega_nt+B_n^*\sin\Omega_nt\right\};\quad \ddot{y}_{\mathrm{g}}^*(t)=e_y(t)\left\{\sum_{n=1}^{N_{\mathrm{f}}}C_n^*\cos\Omega_nt+D_n^*\sin\Omega_nt\right\} \tag{26}$$

  Here, $\{A_i^*,B_i^*,C_i^*,D_i^*\}_{i=1}^{N_{\mathrm{f}}}$ correspond to the point in the original space of random variables to which the check point in the standard normal space gets mapped.
- A vector $\{\gamma_i\}_{i=1}^{4N_{\mathrm{f}}}$, which is a measure of sensitivity of reliability index with respect to individual random variables $\{A_i,B_i,C_i,D_i\}_{i=1}^{N_{\mathrm{f}}}$ evaluated at the check point [43].

It is believed that the above descriptors are of significant interest in modelling the optimal earthquake inputs. Finally, we wish to add that the procedure developed herein has the inherent capability to take into account any uncertainties that may exist in specifying the structure properties as well as permissible response levels.

5. Numerical results and discussion

For the purpose of illustrating the formulations developed in the previous two sections, a tall reinforced concrete chimney is considered (see Fig. 1). The chimney is taken to have uniform circular cross-section of 3.80 m outer diameter, 3.30 m inner diameter, constant mass density of 2500 kg/m^3 and modulus of elasticity $E=2.0\times10^{10}$ N/m^2. Furthermore, the structure is taken to be acted upon by a horizontal and a vertical

ground acceleration and is assumed to be located on a firm soil site. According to Eq. (8), the first five natural frequencies of the chimney were computed to be 0.94, 5.90, 16.52, 32.36 and 53.51 Hz. Since, the frequency bandwidth of ground accelerations is taken as (0–25.00) Hz, the first three natural frequencies of the chimney are only retained in the dynamic analysis. The damping coefficient is taken to be 5% for all the three modes.

5.1. Description of constraints

A set of 10 earthquake records is used in quantifying the constraints for the probabilistic critical excitations. These records include digitized data on acceleration, velocity and displacement and are measured on a firm soil site [44,45]. The details of these records are provided in Table 1. Based on an analysis of these records, the following quantities are determined $E_{0x} = 1.45\ \mathrm{m^2/s^4}$ and $E_{0y} = 1.21\ \mathrm{m^2/s^4}$. The dominant input frequencies are taken to be $n_{0x}^{+} = 1.64/\mathrm{s}$ and $n_{0y}^{+} = 1.72/\mathrm{s}$. Based on these values, E_{2x} and E_{2y} were computed to be $153.96\ \mathrm{m^2/s^6}$ and $141.32\ \mathrm{m^2/s^6}$, respectively. This, in turn, implies that the expected peak values of $\ddot{x}_{\mathrm{g}}(t)$ and $\ddot{y}_{\mathrm{g}}(t)$ are, respectively, $4.35\ \mathrm{m/s^2}$ (0.44 g) and $4.10\ \mathrm{m/s^2}$ (0.42 g). The increases of entropy rate for horizontal and vertical ground accelerations from a reference white noise of intensity $0.02\ \mathrm{m^2/s^3}$ were computed to be $\Delta\overline{H}_{Wx} = 0.10$ and $\Delta\overline{H}_{Wy} = 0.09$, respectively. The parameters in the convergence criteria for the β_{HL} algorithm were taken to be $\delta_1 = \delta_2 = 0.001$ and $\delta_3 = 10^{-6}$ and the constant f is taken as 3. In the numerical calculations it is assumed that the frequency range for both the acceleration components is (0–25.00) Hz and $N_{\mathrm{f}} = 31$. Accordingly, the total number of random variables involved in computing probabilistic critical excitations is 124 ($4N_{\mathrm{f}}$). While distributing the earthquake frequencies Ω_n, $n = 1, 2, \ldots, N_{\mathrm{f}}$, of the series representation of Eq. (11) in the interval $(\omega_0, \omega_{\mathrm{c}})$ it was found advantageous to select some of these Ω_i to coincide exactly with the structure natural frequencies that lie in $(\omega_0, \omega_{\mathrm{c}})$ and also to place relatively more points within the modal half-power bandwidths. Thus, the set of input frequencies $\{\Omega_n\}_{n=1}^{N_{\mathrm{f}}}$ in the series representations (see Eq. (11)) were chosen such that discrete harmonic components were present at ω_1, $2\omega_1$, ω_2, $2\omega_2$ and ω_3, where ω_1, ω_2 and ω_3, are the first three natural frequencies of the chimney. The parameters of the envelope functions are taken to be $\alpha_{x_1} = 0.13$, $\alpha_{x_2} = 0.50$, $A_{0x} = 2.17$, $\alpha_{y_1} = 0.13$, $\alpha_{y_2} = 0.50$ and $A_{0y} = 2.17$. This implies a duration of about 30 s for the horizontal and vertical acceleration components. The numerical integration is carried out using the Wilson-θ method, and the parameter θ was taken as 1.40, with a time step $\Delta t = 0.005$ s.

5.2. Results and discussion

For the purpose of illustration we determine critical excitations by considering two possible cases of constraints: in case 1, constraints on $E_x, E_y, n_{0x}^{+}, n_{0y}^{+}, \sigma_{AC}$ and σ_{AD} are imposed; in case 2, additional constraints on $\Delta\overline{H}_{Wx}$ and $\Delta\overline{H}_{Wy}$ are also imposed. A separate study of these two cases affords insights into the role played by constraints on input entropy rates in the determination of critical psd functions. The failure criterion chosen for defining the performance function of Eq. (15) is taken as the tip relative displacement of the chimney. Accordingly, the resistance, R, of Eq. (15), is taken as the maximum permissible tip relative displacement. In the numerical calculation, R is taken to be $h/75 = 0.6133$ m. In each case, after determining the critical input psd matrix, we carry out a 1000 samples Monte Carlo simulations to estimate the statistics of response processes of interest. The question on the number of terms to be retained in the series representation of $\ddot{x}_{\mathrm{g}}(t)$ and $\ddot{y}_{\mathrm{g}}(t)$ on the convergence of critical reliability indices, β_{HL}, was studied and a value of $N_{\mathrm{f}} = 31$ was seen to give a satisfactory representation.

The calculation of β_{HL} in the present study is based on the use of response surface modelling. For the method to be successful it is required that:

(a) The failure surface in the transformed standard normal space does not possess more than one region which makes comparable contributions to the failure probability, and
(b) The response surface provides an acceptable fit to the failure surface near the failure point

For the problem on hand, it is difficult to prove that these conditions are invariably met for all choices of the parameters of the problem. However, for specific cases limited verifications are possible. To illustrate this, we consider the case when only a stationary horizontal component of earthquake excitation acts on the struc-

Table 1
Information on basis earthquake records for a firm soil site [44,45]

Serial No.	Earthquake	Site	Richter's magnitude	Epicentre distance (km)	Component	PGA (m/s^2)	PGV (m)	PGD(m/s)	Energy[a] (m/s$^{1.5}$)
1	Mamoth lakes	Convict Greek			W	4.02	0.21	0.05	3.73
	05.25.1980		6.2	1.5	UP	3.78	0.21	0.07	2.75
2	Loma prieta	Capitola			W	3.91	0.31	0.07	3.82
	10.18.1989		7.0	9.7	UP	2.50	0.19	0.05	2.58
3	Morgan hill	Halls valley			S60E	3.06	0.40	0.07	2.33
	04.24.1984		6.1	4.5	UP	1.08	0.12	0.01	1.16
4	San Fernando	Castaic, old ridge route			N21E	3.09	0.17	0.04	2.07
	02.09.1971		6.6	27.6	UP	1.53	0.06	0.04	1.29
5	Parkfield	Parkfield fault zone			N	3.80	0.10	0.01	1.74
	12.20.1994		5.0	9.1	UP	1.56	0.03	0.01	0.76
6	Caolinga	Cantua creek school			N	2.83	0.26	0.10	2.67
	05.02.1983		6.5	30.1	UP	1.03	0.06	0.04	1.23
7	Northridge	Cangoa park			S16W	3.81	0.60	0.12	4.17
	01.17.1994		6.7	5.9	UP	4.10	0.14	0.03	3.03
8	Cape Mendocino	Petrolia general store			N	3.25	0.45	0.15	2.44
	04.25.1992		7.0	5.4	UP	1.80	0.21	0.14	1.57
9	Westmorland	Westmorland fire station			S	4.35	0.44	0.15	3.26
	04.26.1981		5.0	6.6	UP	2.68	0.26	0.13	1.61
10	Imperial valley	Calexico fire station			S45W	2.68	0.22	0.10	2.30
	10.15.1979		6.4	17.4	UP	1.71	0.04	0.01	1.69

[a] Energy $= [\int_0^\infty \ddot{u}_{gn}(t)\mathrm{d}t]^{1/2}$.

ture. In this case the response process is Gaussian in nature and, consequently, the extreme of this process over a specified time duration can be approximated by a Gumbel random variable. This would mean that the probability of failure of the structure, with respect to the performance function, as in Eq. (10), can be determined without taking recourse to response surface modelling. This, in turn, means that the critical psd function here can be determined directly by minimizing P_f without adopting the response surface approach. The '*exact*' results on the critical psd function so obtained is compared in Fig. 2 with corresponding results based on response surface based procedure. The two results show nearly the same behavior. This, at least to a limited extent, verifies the applicability of the response surface approach to the present problem. For the general case when both vertical and horizontal excitation components act simultaneously on the structure, this type of verification is difficult to make. In the present study we proceed with the premise that the results for this general case can be considered acceptable if the results obtained are qualitatively consistent with the known features of the response of parametrically excited systems.

For the more general case of simultaneous action of both vertical and horizontal components of earthquake accelerations, the numerical results on critical psd functions and the associated responses are shown in Figs. 2–7 and Table 2. For sake of comparison, results on critical response moment when only horizontal component acts on the structure are also included in Table 2. Based on the numerical results presented in this study, the following observations can be made:

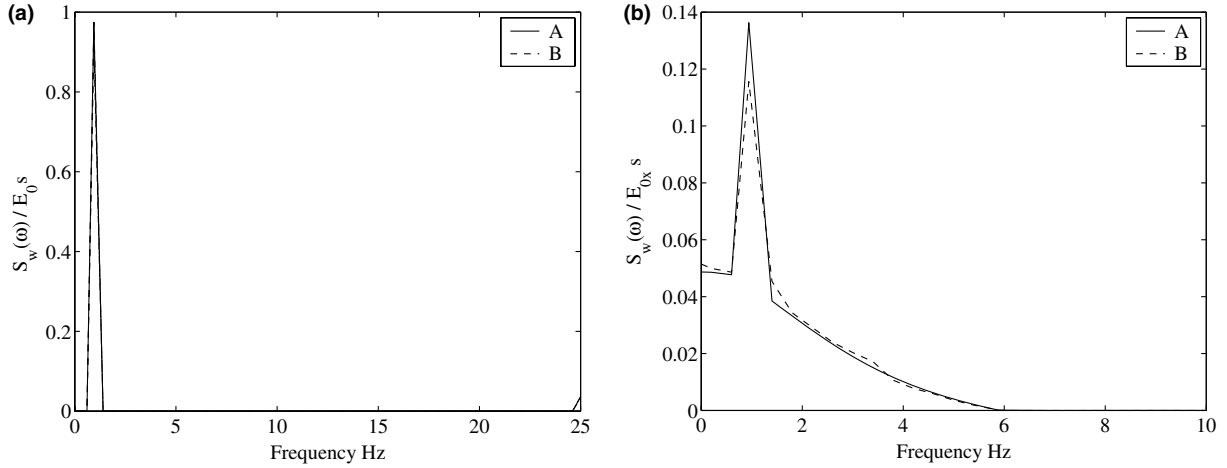

Fig. 2. Critical psd of $\ddot{w}_g(t)$; $\ddot{v}_g(t) = 0$ (a) case 1 (b) case 2, Note: A = objective: to maximize P_f; B = objective: to minimize β_{HL}.

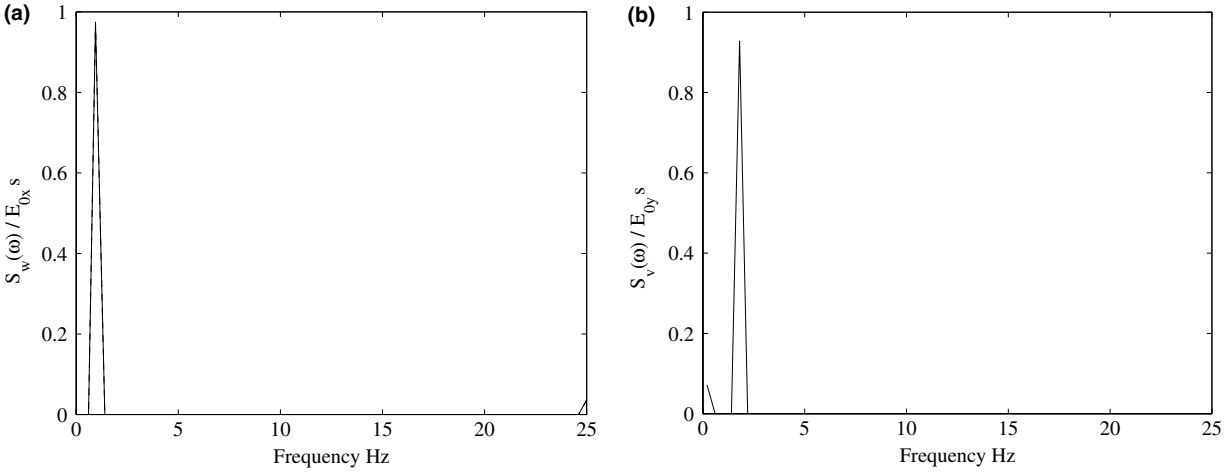

Fig. 3. Case 1: Critical auto-psd functions; (a) $\ddot{w}_g(t)$ and (b) $\ddot{v}_g(t)$.

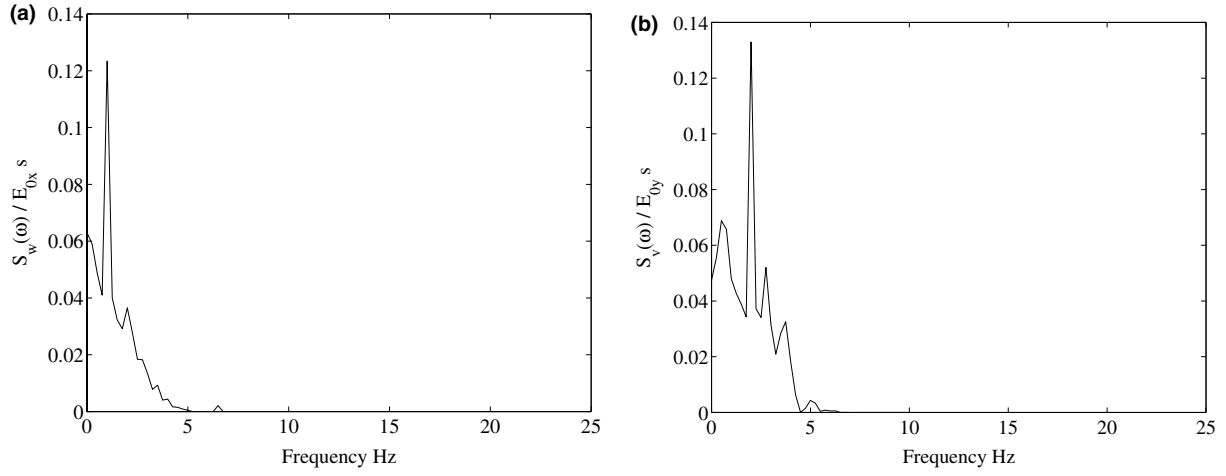

Fig. 4. Case 2: Critical auto-psd functions; (a) $\ddot{w}_g(t)$ and (b) $\ddot{v}_g(t)$.

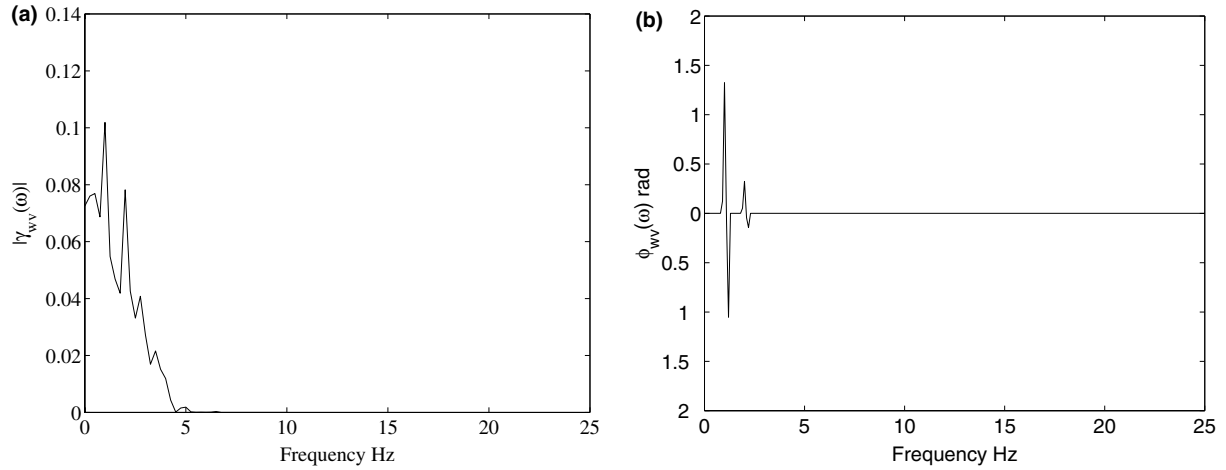

Fig. 5. Case 2: Critical coherency function; (a) amplitude spectrum and (b) phase spectrum.

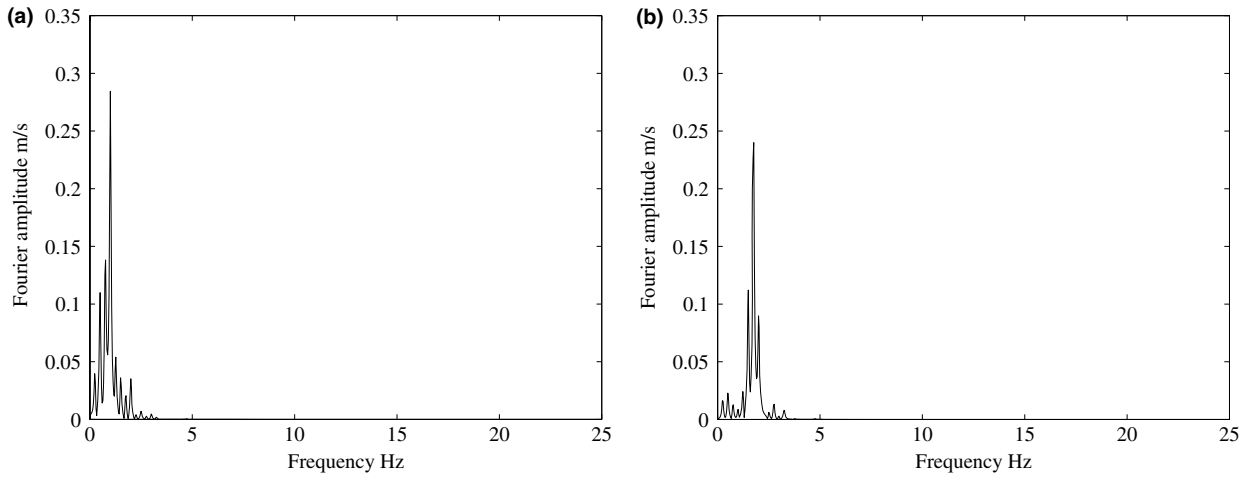

Fig. 6. Case 2: Deterministic input at the check point; (a) $\ddot{x}_g(t)$ and (b) $\ddot{y}_g(t)$.

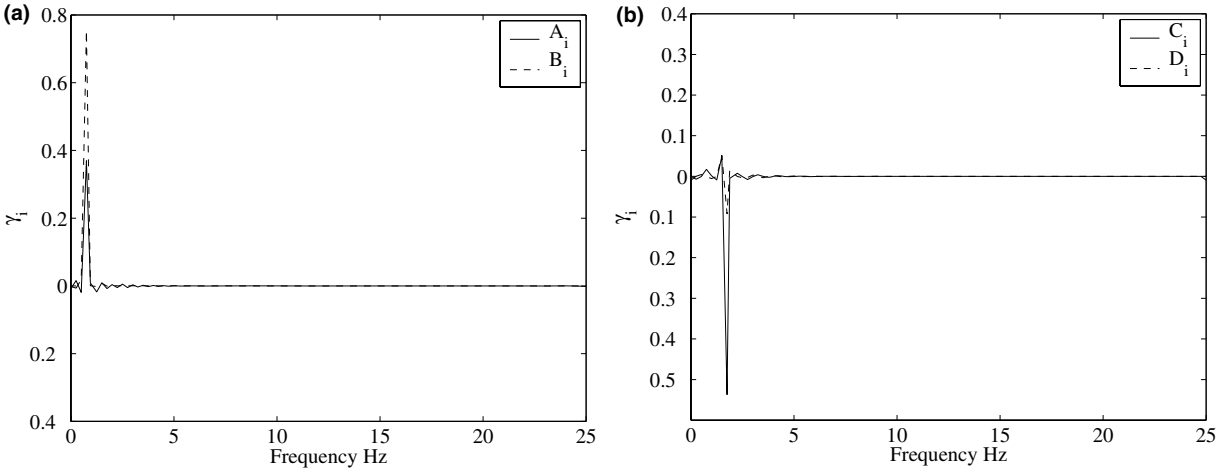

Fig. 7. Case 2: Sensitivity index γ_i; (a) $\ddot{x}_g(t)$ and (b) $\ddot{y}_g(t)$.

Table 2
Summary of maximum responses of the chimney from probabilistic critical inputs

	Vertical excitation absent		Vertical excitation present	
	Case 1	Case 2	Case 1	Case 2
$\mu_{u_{max}}$ (m)	0	0	0.0762	0.0494
$\mu_{BM_{max}}$ (MN m)	0	0	7.8531	5.0746
$\mu_{SF_{max}}$ (MN)	0	0	0.1683	0.0971
$\sigma_{u_{max}}$ (m)	0.4401	0.2479	0.4736	0.2667
$\sigma_{BM_{max}}$ (MN m)	76.0481	37.1812	79.371	39.4327
$\sigma_{SF_{max}}$ (MN)	1.8509	1.0873	1.9615	1.1711

1. If information on future earthquakes is limited to total average energy and zero crossing rate, the critical psd function of the stationary part for both the horizontal and vertical accelerations are highly resonant and critical response produced is conservative (Table 2). It is observed that the power of the psd function for the stationary part of the horizontal acceleration is concentrated at the structure fundamental natural frequency (Fig. 3(a)), and, that for the stationary part of the vertical acceleration is concentrated at a frequency that is twice the structure natural frequency (Fig. 3(b)). This is clearly an indicative of the propensity of the critical excitations to produce parametric resonances in the first structural mode. The imposition of entropy rate constraint, case 2, forces the amplitudes of psd functions to get redistributed across other frequencies, see Fig. 4. However, the vertical acceleration is seen to posses a dominant frequency at twice the structure fundamental natural frequency. The two components of ground accelerations are generally found to be weakly correlated with the correlation being poorer for case 1 than for case 2. Fig. 5 shows the amplitude and phase of critical cross psd function between the critical excitation components for case 2. The reliability index, β_{HL}, was computed to be 2.19 for case 1 and to be 4.23 for case 2. Based on these values, the notional probability of failure is computed respectively to be 1.4262×10^{-2} and 1.1685×10^{-5}. The effect of the entropy rate constraint on reducing the structure response moments peak can be seen in Table 2.
2. When the constraints on entropy rate are imposed (case 2), it is observed that the horizontal ground acceleration, $\ddot{x}_g(t)$, at the check point (see Eq. (26)) possesses a dominant amplitude at the chimney fundamental natural frequency (see Fig. 6(a)). While, the vertical acceleration, $\ddot{y}_g(t)$, has a dominant frequency that is twice the chimney fundamental natural frequency (Fig. 6(b)). Furthermore, maximum responses produced by the pair of deterministic horizontal and vertical time histories at the design point (see Eq. (26)) matches well with corresponding maximum responses from critical input. The peak responses of tip displacement,

base bending moment and shear force were computed to be 0.7295 m, 107.0065 MN m and 3.2021 MN from the deterministic input at the check point and for stochastic critical excitations, these expected peaks were estimated to be 0.7314 m, 107.8361 MN m and 3.2702 MN, respectively. It is to be noted that, maximum responses from critical input were computed using Monte Carlo simulations by averaging the maximum responses across the 1000 samples.

3. The study of the direction cosines of the position vector at the check point revealed that β_{HL} is most sensitive to A_n and B_n that are located near the structural fundamental frequency. Similarly, β_{HL} was also sensitive to C_n and D_n that are located at twice the structure fundamental frequency. These features can be evidenced from Fig. 7.
4. As it can be expected, β_{HL} was seen to increase while P_{f_0} was seen to decrease when the maximum allowable tip relative displacement, R, increases. For example, β_{HL} was computed to be 3.82, 4.04, 4.23, 4.45 and 4.61 when R was taken to be 0.4907, 0.5520, 0.6133, 0.6747 and 0.7360 m, respectively. The associated values of P_{f_0} were 6.6726×10^{-5}, 2.6726×10^{-5}, 1.1685×10^{-5}, 4.2935×10^{-6} and 2.0133×10^{-6}, respectively.
5. Results on probabilistic critical earthquake excitations are found to be sensitive to changes in constraints on horizontal acceleration than changes in constraints on vertical acceleration. The chimney reliability index, β_{HL} was found to be more sensitive to the constraints on entropy rate and energy than constraints on zero crossing rate and envelopes parameters. For example, the percentage changes in β_{HL} were computed to be 0.63, 0.54, 3.11, 0.03 and 0.07 due to changes of 1% in the parameters E_{0x}, n_{0x}^{+}, $\Delta\overline{H}_{Wx}$, α_{x_1} and α_{x_2}, respectively. In computing these percentage changes, each of these parameters was changed one at a time, while holding other parameters fixed to their reference values.
6. To assess the effect of vertical ground acceleration, critical responses are calculated without including the vertical excitations; see Table 2. When vertical excitation is absent, the mean response is zero. The highest root mean square responses without vertical excitations are generally found to be less than the corresponding quantities computed by including the vertical excitation. This difference is about 3% for case 1 and about 15% for case 2.

As has been already noted, the form of the response surface assumed in Eq. (24) does not take into account the cross quadratic terms. With a view to investigate the influence of inclusion of cross terms in the response surface model on the critical response and psd functions, limited studies were conducted. Thus, for the case of simultaneous action of horizontal and vertical nonstationary seismic inputs, with the inclusion of cross terms, the critical β_{HL}, for cases 1 and 2, with interaction terms included, were computed to be 2.13 and 4.11, respectively. These results are marginally different from the corresponding results when the cross terms were excluded, which have already been computed to be 2.19 and 4.13, respectively. Similarly, the changes in critical psd functions were also found to be marginally small. In this context it is to be noted that the fit for the response surface here is obtained in the space of standard normal random variables. This would mean that the mutual dependencies and non-Gaussian nature of the basic random variables are implicitly taken into account in deriving the response surface even when cross terms in the model are not included. This possibly explains the marginal influence that the cross terms in response surface model have on the final outcome of the case studies conducted.

In the evaluation of the structural reliability in this study, the constraints on the input, such as, the total average energy and average zero crossing rate, have been treated as being deterministic in nature. One could treat these quantities also as random variables so that the uncertainties involved in their specification could be quantified. The probability distribution of these variables needs to be obtained based on studies such as site-specific seismic hazard analysis and study of local soil conditions. When these uncertainties are also included, one could derive the critical excitation model by optimizing the failure probability conditioned on these random variables and subsequently deduce the critical excitation models by using the theorems on conditional expectations. Furthermore, it may be noted that in our study we have not imposed any explicit constraints on the shape of the input power spectra. Therefore it would be of interest to see how the Fourier amplitude spectrum of the samples of critical excitations compares with Fourier amplitude spectra of recorded earthquakes. With this in view we have selected 20 samples of recorded accelerograms. This set includes the records listed in Table 1 and also, ten more records from the Kobe 1995 (Japan), Elcentro 1940 (USA), Chichi 1999 (Taiwan), Bhuj 2001 (India), Uttarkashi 1991 (India), Dharmsala 1986 (India), Smart1 1986 (Taiwan), Koc-

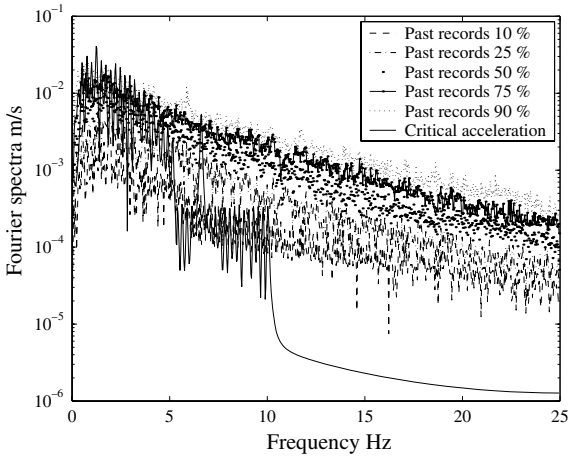

Fig. 8. Fourier amplitude spectrum of sample of critical excitation model as in Fig. 4(a) compared with estimates of exceedance levels obtained from 20 recorded accelerograms.

aeli 1999 (Turkey), Duze 1999 (Turkey) events. Each of these records has been normalized to possess unit peak ground acceleration. Fig. 8 shows the spectrum of 10%, 25%, 50%, 75% and 90% exceedance levels of this ensemble of Fourier amplitude spectra. Also shown in this figure is the Fourier amplitude spectrum of normalized sample of critical excitation derived from model shown in Fig. 4(a). It may be noted that in the neighborhood of structural fundamental frequency the spectrum of the critical excitation lies above the 90% exceedance levels estimated from recorded data. This feature is to be expected given the very fact that critical excitations are optimized to produce highest response in the given structure. From a seismological perspective, it could be argued that earthquake inputs with such highly peaked power spectral density are unlikely to occur given the inelastic attenuation between the seismic source and site and the inelastic properties at the site. Further research work is clearly needed to expand the scope of the present study to take into account these nonlinear effects in the formation of critical inputs.

6. Conclusions

The problem of determining multi-component critical earthquake load models is considered in this study within the probabilistic framework. The study takes into account the complicating feature arising out of the vertical component of ground motion appearing as a parametric term in the governing equation of motion. The development of stochastic critical excitation has involved the exploration of newer concepts and tools. Specifically, the study reported in this paper, to the best of author's knowledge, for the first time, combines concepts from response surface modelling, reliability indices and nonlinear optimization programming in arriving at a vector random critical excitation model that minimizes the structure reliability index. A significant merit of this approach has been that the method leads not only to the definition of critical excitation-response pair, but also, provides valuable information on the nature of excitation at the check point and a vector of sensitivity indices relating the critical reliability index and the excitation parameters. In the illustrative example considered, the critical excitation is shown to capture well the qualitative feature of primary and secondary resonances observed in parametrically excited systems.

References

[1] Ibrahim RA. Parametric random vibration. USA: Wiley; 1985.
[2] Bolotin VV. Random vibrations of elastic systems. Netherlands: Martinus Nishoff Publishers; 1984.
[3] Dimentberg MF. Statistical dynamics of nonlinear and time-varying systems. UK: Wiley; 1988.
[4] Lin YK, Cai CQ. Probabilistic structural dynamics. Singapore: McGraw-Hill, Inc; 1995.
[5] Iyengar RN, Shinozuka M. Effect of self-weight and vertical acceleration on the behavior of tall structures during earthquakes. Earthquake Eng Struct Dyn 1972;1:69–78.

[6] Lin YK, Shih TY. Column response to horizontal-vertical earthquakes. J Eng Mech 1980;106:1099–109.
[7] Lin YK, Shih TY. Vertical seismic load effect on building response. J Eng Mech 1980;107:331–43.
[8] Shih TY, Lin YK. Vertical seismic load effect on hysteretic columns. J Eng Mech 1982;108:242–54.
[9] Shih TY, Chen YC. Stochastic earthquake response of tapered column. J Eng Mech 1984;110:1185–210.
[10] Ahmadi G. Bounds on earthquake response of structures. J Eng Mech 1985;112:351–69.
[11] Ahmadi G, Abdel-Rahman S. Stability of elastic frames subjected to earthquake excitations. Earthquake Eng Struct Dyn 1986;14:455–74.
[12] Loh CH, Ma MJ. Reliability assessment of structure subjected to horizontal–vertical random earthquake excitations. Struct Safety 1997;19:153–68.
[13] Drenick RF. Model-free design of aseismic structures. J Eng Mech 1970;96:483–93.
[14] Shinozuka M. Maximum structural response to seismic excitations. J Eng Mech 1970;96:729–38.
[15] Iyengar RN. Matched inputs. Report 47, Series J. Center of Applied Stochastics, Purdue University, West Lafayette, IN; 1970.
[16] Iyengar RN, Manohar CS. Nonstationary random critical excitations. J Eng Mech 1987;133:529–41.
[17] Srinivasan M, Corotis R, Ellingwood B. Generation of critical stochastic earthquakes. Earthquake Eng. Struct Dyn 1992;21:275–88.
[18] Manohar CS, Sarkar A. Critical earthquake input power spectral density function models for engineering structures. Earthquake Eng Struct Dyn 1995;24:1549–66.
[19] Abbas AM, Manohar CS. Investigations into critical earthquake load models within deterministic and probabilistic frameworks. Earthquake Eng Struct Dyn 2002;31:813–32.
[20] Takewaki I. A new method for non-stationary random critical excitation. Earthquake Eng Struct Dyn 2001;30:519–35.
[21] Takewaki I. Probabilistic critical excitation for MDOF elastic–plastic structures on compliant ground. Earthquake Eng Struct Dyn 2001;30:1345–60.
[22] Sarkar A, Manohar CS. Critical cross power spectral density functions and the highest response of multi-supported structures to multi component earthquake excitations. Earthquake Eng Struct Dyn 1996;25:303–15.
[23] Sarkar A, Manohar CS. Critical seismic vector random excitations for multi-supported structures. J Sound Vibrat 1998;212:525–46.
[24] Abbas AM, Manohar CS. Critical spatially varying earthquake load models for extended structures. J Struct Eng 2002;29:39–52.
[25] Sarkar A, Khajehpour S. Response level crossing rate of a linear system excited by a partially specified Gaussian load process. Probabilistic Eng Mech 2001;17:85–95.
[26] Abbas AM, Manohar CS. Reliability-based critical earthquake load models, Part I: Linear structures. J Sound Vibrat 2005;287:865–82.
[27] Abbas AM, Manohar CS. Reliability-based critical earthquake load models, Part II: Nonlinear structures. J Sound Vibrat 2005;287:883–900.
[28] Iyengar RN, Dash PK. Random vibration analysis of stochastic time-varying systems. J Sound Vibrat 1976;45:69–89.
[29] Finlayson BV. Method of weighted residuals and variational principles. New York: Academic Press; 1972.
[30] Flatto L. Advanced calculus. Baltimore: The Williams and Wilkins Company; 1976.
[31] Blevins RD. Formulas for natural frequency and mode shape. New York: Litton Educational Publishing Inc.; 1979.
[32] Faravelli L. Response-surface approach for reliability analysis. J Eng Mech 1989;115:2763–81.
[33] Bucher CG, Bourgund U. A fast and efficient response surface approach for structural reliability problem. Struct Safety 1990;7:57–66.
[34] Rajashekhar MR, Ellingwood BR. A new look at the response surface approach for reliability analysis. Struct Safety 1994;12:205–20.
[35] Papoulis A, Pillai SU. Probability, random variables and stochastic processes. Boston: McGraw Hill; 2002.
[36] Kapur JN. Maximum entropy models in science and engineering. New Dehli: Wiley Eastern; 1993.
[37] Brune JN. Tectonic stress and the spectra of seismic shear waves from earthquakes. J Geophys Res 1970;75:4997–5009.
[38] Hanks TG, McGuire RK. The character of high frequency ground motions based on seismic shear waves. Bull Seismol Soc Am 1981;71:2071–95.
[39] Boore DM. Stochastic simulation of high-frequency ground motions based on seismological models of the radiated spectra. Bull Seismol Soc Am 1983;73:1865–94.
[40] Quek ST, Teo YP, Balendra T. Non-stationary structural response with evolutionary spectra using seismological input model. Earthquake Eng Struct Dyn 1990;19:275–88.
[41] Hasofer AM, Lind N. An exact and invariant first-order reliability format. J Eng Mech 1974;100:111–21.
[42] Ang AH-S, Tang WH. Probability concepts in engineering planning and design: Vol. II Decision risk and reliability. USA: Wiley; 1984.
[43] Kiureghian AD, Ke J-B. Finite-element based reliability analysis of frame structures. In: Proceedings of the International Conference on Structural Safety and Reliability (ICOSSAR) Kobe, Japan, vol. 1, 1985. p. 395–404.
[44] Shakal AF, Huang MJ. Standard tape format for CSMIP strong-motion data tapes. California strong motion instrumentation program. Report OSMS 1985; 85–03.
[45] SMDB. The Strong Motion Databased. http://smdb.crustal.ucsb.edu/, Southern California Earthquake Center 2000.